ICAS-88-3.4.2

FATIGUE LIFE IMPROVEMENT OF THICK SECTIONS BY HOLE COLD EXPANSION

J.Y. Mann; P.W. Beaver and J.G. Sparrow
Aircraft Structures Division, Aeronautical Research Laboratory,
Melbourne, Victoria,
Australia

Abstract

Flight-by-flight fatigue tests were carried out on flat specimens of A7-U4SG-T651 (2214-T651) aluminium alloy of thickness between 8 and 30 mm which incorporated open holes of about 8.5 mm in diameter, either reamed or cold-expanded using a tapered mandrel. A comprehensive study was made of the deformation characteristics of the holes during and after cold expansion, and this was supported by fractographic studies of crack initiation and propagation. Evidence is presented to show that there are differences (which are thickness dependent) in the deformation characteristics of the material at the mandrel entry and exit ends of the hole and that these influence the sequence of fatigue crack initiation along the hole and the subsequent shape of the fatigue crack as it propagates through the section. Residual strength tests on cracked cold-expanded hole specimens suggest that the critical size of the crack is greater than for simple non-cold-expanded hole specimens. This finding and the information relating to crack growth rates has some important implications for the implementation of damage tolerance philosophies in structures incorporating cold-expanded holes.

I. INTRODUCTION

The cold expansion of circular holes, subsequently either left open or filled with fasteners, is now a common technique for increasing the fatigue lives of aircraft structural members. Perhaps the most widely used commercially available hole cold-expansion process is that developed in the early 1970's by the Boeing Commerical Airplane Company[1] and now marketed by Fatigue Technology Inc. (FTI), Seattle, USA. This process involves the pulling of an oversize tapered steel mandrel through a hole containing a thin internally-lubricated stainless steel split sleeve, to provide a plastic radial expansion of between 3% and 7%. As a consequence, a compressive residual hoop stress field is developed in the material adjacent to the hole which, in turn, is balanced by a more remote tensile stress field[2].

Most aircraft structural applications of the split-sleeve cold-expansion process have involved either sheet or plate of up to about 12 mm in thickness (with holes of from 5 to 8 mm in diameter); or lugs which, although in thicknesses of up to 35 mm, have had correspondingly large hole diameters, e.g. 25 to 30 mm. In most cases the hole aspect ratio (i.e. hole length/hole diameter) has been less that 1.5.

In 1978 a requirement arose to extend the fatigue life of the wing main spar of the Mirage IIIO fighter operated by the Royal Australian Air Force. The flange thickness in the areas of interest was between 20 and 33 mm, and the fastener holes between 5 and 10 mm in diameter[3,4]. Typically, the hole aspect ratio was greater than three. Cold expansion of holes using the split-sleeve process was one of the techniques used to increase the service life[5,6], and the same process was used to improve the fatigue performance of the Kfir fighter wing[7]. Associated Australian investigations[8,9] which involved specimens of 15 and 23 mm thickness with 8.5 mm holes, indicated some unusual asymmetric through-thickness crack development characteristics, in that the crack dimensions were much greater at the face corresponding to the entry of the cold-expansion mandrel than at the exit face, giving rise to what was designated a "bulbous nose" fracture. Somewhat similar fracture characteristics have been reported by other investigators[10,11].

This paper covers a more extensive investigation into the effects of material thickness on the deformation characteristics and fatigue fracture development associated with cold-expanded holes in material ranging in thickness from 8 to 30 mm. It also provides some information relating to the residual strength of cold-expanded hole specimens containing fatigue cracks.

II. TEST SPECIMENS AND COLD-EXPANSION CONDITIONS

Test specimens used in these investigations were made from several plates of a batch of 55 mm thick A7-U4SG (2214) aluminium alloy, which was given the ARL serial code JP. Table 1 gives the average static tensile properties of four specimens machined from plates JP5 and JP6. The material 'JP' was received in the -T351 temper condition. Specimen blanks were aged to the -T651 condition by heat treating at 160^{o} +/- 3^{o}C for 20 hours.

	Specification A7-U4SG-T651 (2214-T651)	Test material
0.1% proof stress (MPa)	-	433.0
0.2% proof stress (MPa)	390	437.7
Ultimate tensile stress (MPa)	450	491.0
Elongation (%) (5.65 $\sqrt{A}$)	5	10.8

TABLE 1. Properties of test material

Fatigue specimens having the plan form shown in Figure 1 and thicknesses of 8, 15, 23 and 30 mm were used in this investigation. Two combinations of specimen thickness of 30 and 8 mm, and 23 and 15 mm respectively were taken in the through-thickness direction of the 55 mm thick plates. All specimens had their longitudinal axes parallel with the rolling direction of the plates.

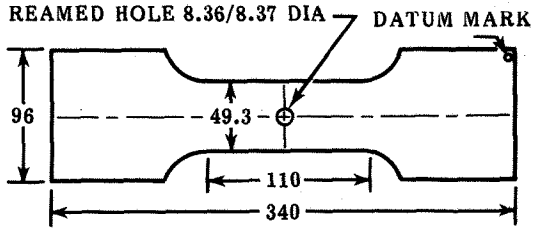

FIGURE 1. Fatigue test specimen

Cold expansion was carried out using FTI tooling including both a hydraulic puller (mainly for the fatigue specimens) and a small HP-20 mechanical hand puller unit for tests involving the determination of strains. In all cases the reamed (pre-expansion) starting-hole size was 8.36/8.37 mm diameter; the mandrel was type CMB-10-2-N-1-20-VI and the sleeves type 10-2-N-23F. This combination of hole starting size, mandrel and sleeve type provided a nominal cold expansion of 4.0% to 4.2%. The split in the sleeve was always oriented on the 'rolling direction' axis of the hole, and the 'Datum Mark' face of the specimen corresponded to the exit of the cold-expansion mandrel.

Prior to hole cold expansion the faces and sides of the specimens were polished using 800 grade paper. However, after cold expansion no further reaming of the holes was carried out, nor was the z-direction displacement on the faces adjacent to the holes removed.

III. TESTING PROGRAMME AND RESULTS

Fatigue tests

All specimens were fatigue tested in axial loading in a servo-controlled electro-hydraulic machine under the simplified 100-flight flight-by-flight loading sequence shown in Figure 2 and summarised in Table 2. This was a simplified version of a Mirage fighter spectrum[12]. In this sequence there is a linear relationship between stress and 'g', and in this particular investigation the maximum load level of the sequence (+7.5g) corresponded to a gross-area stress of 260 MPa, i.e. 1g = 34.7 MPa. In these tests one 100-flight sequence of 1989 cycles took about seven minutes of testing time.

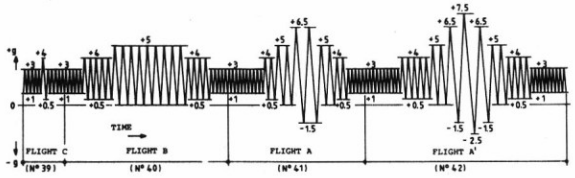

FIGURE 2. Flight types in 100-flight sequence

Loading condition	Cycles (per flight) Type A'	Type A	Type B	Type C	Cycles per 100 flights
+7.5g to -2.5g	1	-	-	-	1
+6.5g to -1.5g	2	2	-	-	38
+5.0g to 0g	4	4	9	-	400
+4.0g to +0.5g	9	4	9	1	450
+3.0g to +1.0g	20	15	10	10	1100
					1989
Flights per 100 flights	1	18	36	45	

TABLE 2. Flight-by-flight loading conditions

The fatigue testing programme for each of the four thicknesses of specimen (i.e. 8, 15, 23 and 30 mm) included control groups (without cold-expanded holes) and those with holes cold expanded as described above. Usually, four specimens were tested under each combination of conditions, the order of testing among the eight groups being pseudo random.

Table 3 gives the individual fatigue test results together with log. average values of lives and standard deviations of log. life in each case. The significance of the lives to failure being predominantly associated with flight 42 is that this flight contains the maximum tensile load which occurs only once in each 100-flight sequence.

Specimen number and flights to failure				log. average life (flights)	s.d. of log. life
8 mm thick non-cold expanded					
JP5E2	JP5A2	JP5J2	JP6C2		
2890	2942	3135	3260	3053	0.024
8 mm tnick cold expanded					
JP6J2	JP5C2	JP6A2	JP6E2		
12242	12342	12442	12642	12416	0.006
15 mm thick non-cold expanded					
JP6F2	JP6B2	JP5H2	JP5D2		
2606	2642	2687	2692	2657	0.007
15 mm thick cold expanded					
JP5K2	JP6H2	JP5F2	JP5B2		
13842	14842	16542	18342	15801	0.054
23 mm thick non-cold expanded					
JP6D1	JP6H1	JP5B1	JP5K1		
2527	2542	2642	2742	2612	0.016
23 mm thick cold expanded					
JP5F1	JP5H1	JP6B1	JP5D1		
15042	15142	15342	16242		
JP6F1	JP6K1			15715	0.017
16242	16342				
30 mm thick non-cold expanded					
JP5G1	JP6J1	JP6A1	JP5C1		
2142	2742	3142	3242	2781	0.082
30 mm thick cold expanded					
JP5A1	JP6C1	JP6G1	JP5E1		
13542	14342	14642	15842	14569	0.028

TABLE 3. Fatigue test results

Fatigue fractures representative of the eight groups of specimens are shown in Figures 3 and 4.

The fracture surfaces of all specimens (both non-cold expanded hole and cold-expanded hole) provided clear evidence of multiple crack initiation on both sides of the hole and through the thickness. In the non-cold-expanded specimens the maximum crack depths did not occur at the faces of the specimens - for specimens of 8, 15 and 23 mm thickness, fatigue crack development was approximately symmetric in both the thickness and transverse directions, while in specimens of 30 mm thickness there was a greater tendency for the maximum

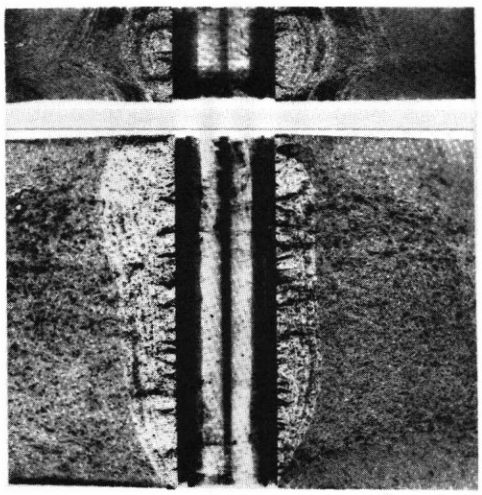

FIGURE 3. Fatigue fractures of non-cold-expanded hole specimens of thickness 8 and 30 mm

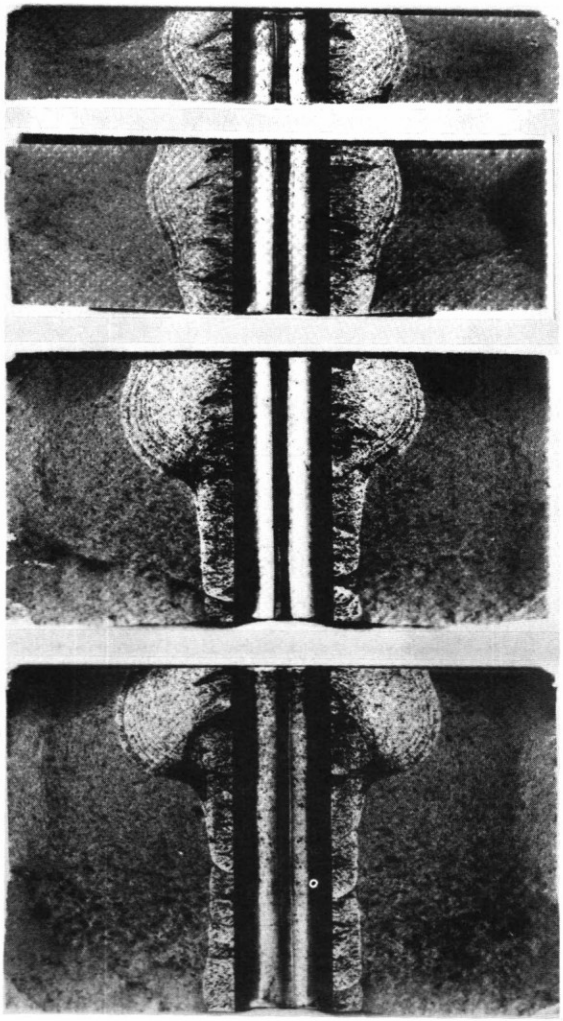

FIGURE 4. Fatigue fractures of cold-expanded hole specimens of 8, 15, 23 and 30 mm thickness, mandrel entry faces at top

crack depth to be closer to one of the faces (Fig. 3(a)). There was clear evidence of "plane stress" tunnelling (Fig. 3(b)) in the 8 mm thick specimens, a feature which became progressively less apparent in the thicker specimens.

The bulbous nose feature in cold-expanded-hole specimens becomes increasingly obvious as the thickness increases from 15 to 30 mm. In the 8 mm thick specimens the feature is not as obvious, and without the evidence from the thicker specimens might not be recognized. Another interesting feature is that (at final fracture) the maximum crack depth of the bulbous nose does not occur at the entry face, but at a position down the hole. For each of the four thicknesses, the average values of the maximum crack depth and the distance from the entry face are given in Table 4.

Thickness (mm)	Distance from entry face (mm)	Maximum crack depth (mm)	Fatigue crack area (% of) gross	nett
8	3.68	7.45	16.4	19.8
15	3.93	6.50	13.3	16.1
23	4.56	9.26	13.0	15.7
30	4.91	9.20	11.8	14.3

TABLE 4. Dimensions of bulbous nose

Fracture toughness tests

Six offcuts from the end of broken 30 mm thick specimens (three from plate JP5 and three from plate JP6) were used to manufacture 24 compact tension fracture toughness specimens of thickness 9.5, 12.5, 19 and 25 mm. The fracture toughness specimens were taken from the offcuts in the L-T direction, i.e. so that the crack growth direction was the same as for the parent fatigue specimens. The results of the fracture toughness tests are given in Table 5.

Thickness (mm)	No. of valid results	Fracture toughness (MPa.m$^{1/2}$) average	std deviation
9.5	6	29.8	0.5
12.5	6	28.7	0.7
19.0	3	32.2	0.9
25.0	6	31.3	1.0

TABLE 5. Fracture toughness results

Within the range of thicknesses given in Table 5 the fracture toughness results do not indicate any conclusive evidence of the expected transition from plane stress to plane strain conditions. It should be noted that the 9.5 mm thickness results do not meet the thickness requirement $B \geq 2.5 (K_Q/\sigma_{ys})^2$.

Displacement and strain measurements

Offcuts from the ends of broken fatigue specimens of each of the four thicknesses were used to measure both the z-direction displacements at the two faces and the strains induced at the inlet face during both the passage of the cold-expansion mandrel through the hole and after its withdrawal. In the first case the hydraulic puller was used, while in the second case the mechanical puller was used.

Displacement measurements were made along a transverse diameter using the focus control on a Zeiss metallurgical microscope at 500X magnification. The results of these measurements are shown in Figure 5.

Strips of miniature electrical-resistance strain gauges were fitted along the transverse diameter of four specimens, one strip of ten gauges on one side of the hole to measure hoop strains, and another of ten on the other side to measure radial strains. The gauges used were HBM KY23 (hoop) and KY13 (radial) which had gauge lengths of 0.8 and 0.6 mm respectively and grid centre line distances of 1.0 mm. In both cases the distances from the edge of the hole to the centre of the first gauge was approximately 0.6 mm. Gauge outputs were fed into a 20-channel strain gauge conditioning box under the control of an HP3497A Data Acquisition/Control Unit. Data processing was done using an HP9816 computer and the strain outputs recorded on an HP7098 multi-channel plotter.

During the cold expansion, the gauged face was oriented to correspond to the mandrel entrance face of the specimen. Commencing from a zero strain datum position, successive readings were taken at increments of 1.27 mm (0.05 inch) (representing one turn of the puller loading screw), until the mandrel had completely passed through the hole. Some illustrative examples of the results of these hoop and radial strain measurements are

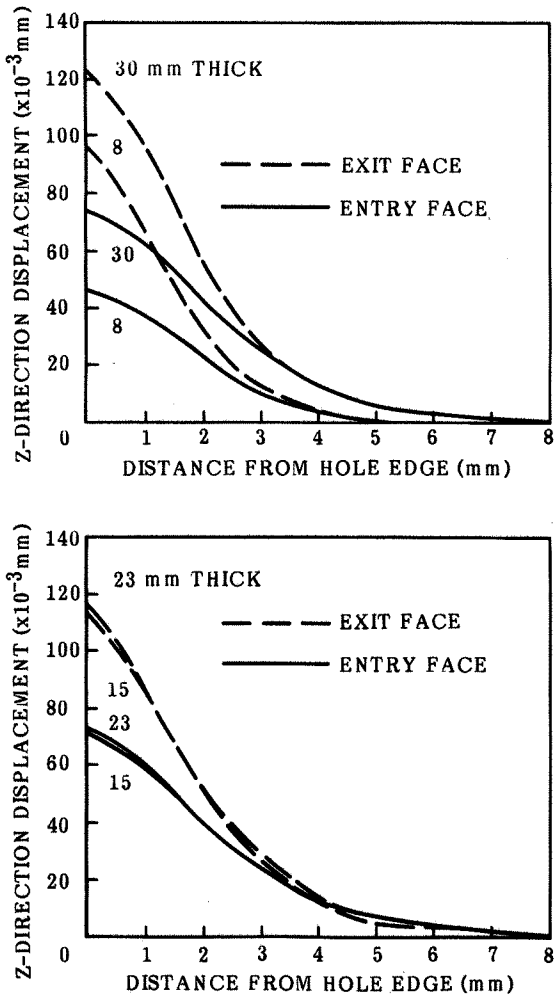

FIGURE 5. Z-direction displacements on faces, cold-expanded holes of 8.4 mm diameter

given in Figure 6. For clarity the plots are shown only for gauges at 0.6, 1.6, 2.6, 3.6, 6.6, and 9.6 mm from the hole. The corresponding gauge numbers are 1,2,3,4, 7 and 10 respectively.

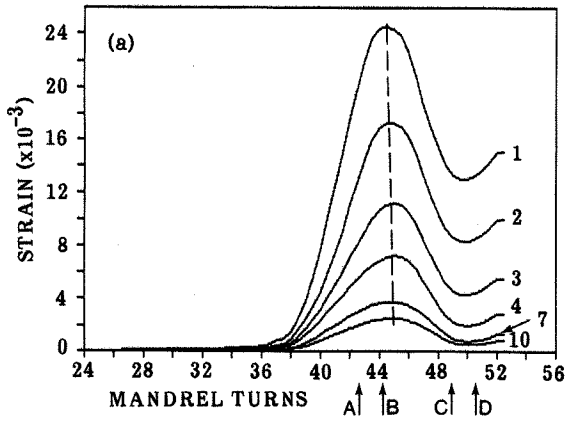

FIGURE 6(a). Strains induced on entry face 8 mm thick specimens, hoop strains

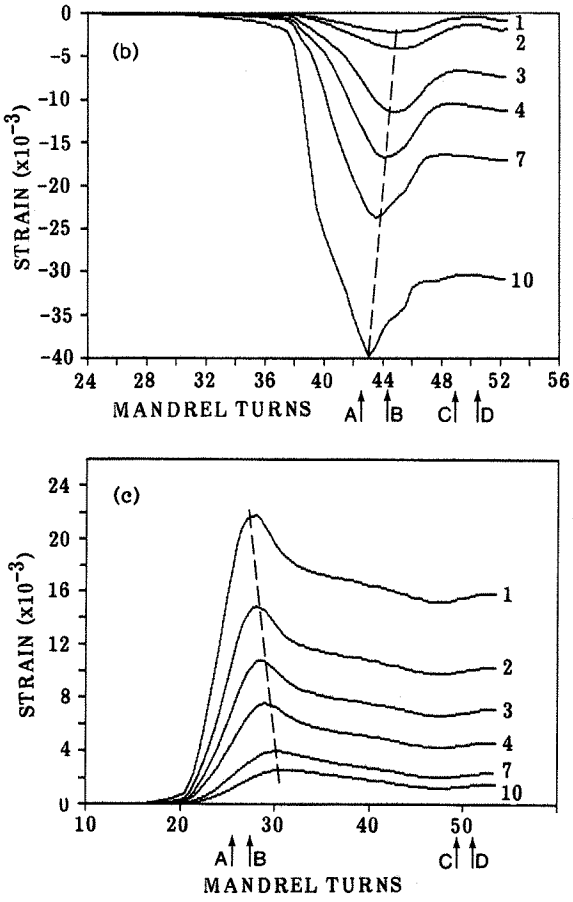

FIGURE 6. Strains induced on entry face
(b) 8 mm thick specimens, radial strains
(c) 30 mm thick specimens, hoop strains

Microhardness measurements and grain flow around cold-expanded holes

Microhardness measurements have been used to indicate the amount of plastic deformation resulting from mechanical processes such as drilling and reaming of holes[13] and shot peening[14]. This technique has also been used to measure the extent of plastic deformation adjacent to cold-expanded holes[15], where some change in hardness was observed within about 1 mm of the hole. In the current work two specimens were examined by this method, both after optically polishing the faces to remove the z-direction displacements. One was in 8 mm thick material and incorporated the same size hole as referred to above, while the other was in 30 mm thick material and incorporated a hole of approximately 21 mm diameter which had also been cold-expanded using the split-sleeve process. However, in both cases no changes in the microhardness values were observed for distances of between about 0.05 mm and 12.0 mm from the edge of the cold-expanded holes.

It is also possible to delineate high plastic strain regions in some commercial Al-Mg and Al-Cu-Mg alloys by decorating the regions of high strain using a low temperature precipitation and etching technique[16]. This technique was used to examine the flow patterns through the thickness of some cold-expanded hole specimens. However, no apparent changes in the grain structure around the holes was observed in the 8 and 30 mm thick specimens which were examined.

Residual static strength

Fatigue tests were carried out on a group of 15 mm thick specimens taken from plate JP4 which included seven with non-cold-expanded holes and eight with cold-expanded holes. They were fatigue tested under the same loading condtions as used previously, but to nominated percentages of their nominal average lives to failure, based on the results of tests reported in Reference 9. In this instance the average life to failure of the non-cold expanded specimens were 2442 flights, and that of the cold-expanded specimens 16765 flights.

After fatigue cracking, the specimens were loaded in tension at a rate of 75 - 100 kN per minute until fracture occurred. The results are given in Table 6.

Specimen no.	Life (% of average)	Flights	Residual strength (kN)	Fatigue crack area (mm^2)
Non-cold-expanded				
JP4C2	0	0	284.3	0
JP4B1	40	1000	278.4	1.3
JP4H1	50	1200	264.2	3.3
JP4F2	60	1500	269.0	3.4
JP4A2	70	1700	266.6	3.2
JP4E1	80	2000	231.0	15.6
JP4K2	90	2200	266.6	4.5
Cold-expanded				
JP4H2	0	0	296.2	0
JP4J2	20	3400	260.6	7.9
JP4A1	30	5000	207.3	89.0
JP4E2	40	6700	225.1	41.5
JP4D1	50	8400	225.1	54.8
JP4K1	60	10100	201.4	57.1
JP4G1	70	11700	222.7	60.0
JP4B2	80	13400	219.2	69.3

TABLE 6. Results of residual strength tests

In addition to providing residual strength data, these specimens enabled a fractographic study to be made of the early stages of fatigue crack development.

Fractographic crack propagation measurements

The results of fractographic crack propagation studies on 15 mm thick specimens fatigue tested under identical conditions to those in this paper will be reported elsewhere[17]. These included a cold-expanded hole specimen - JP2A2 with a life of 16442 flights - which had a similar fracture appearance to the 15 mm thick specimen shown in Figure 4. Two traverses were made perpendicular to the hole, one at the bulbous nose (mandrel entry) end corresponding to the deepest part of the final crack front and the other near the mandrel exit end of the hole approximately 1.9 mm from the face. The 'marker' used to identify crack growth increments was the fatigue striation and/or the band of tensile crack extension produced by the highest tensile load in the sequence which occurred in flight 42. Figure 7 shows the resulting crack propagation curves. For the crack near the mandrel entry face the crack depth at which measurements commenced was 0.046 mm, while for that near the mandrel exit face the depth was 0.184 mm.

IV. DISCUSSION

Cold expansion of the holes resulted in a significant increase in the lives of specimens of all four thicknesses of material. However, the increase in life was less for 8 mm thick specimens compared with those of the other thicknesses - 4:1 against 6:1 relative to non-cold-

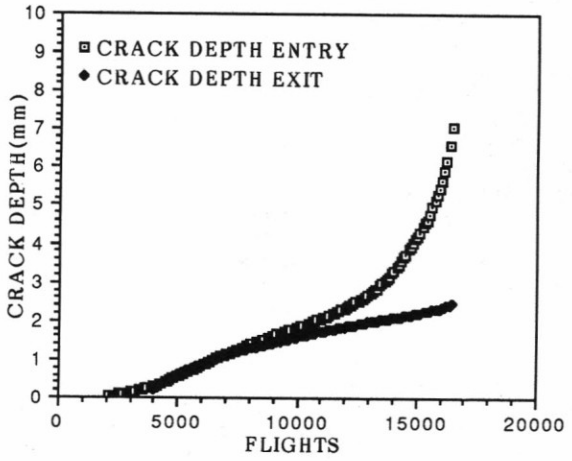

FIGURE 7. Fatigue crack propagation curves for cold-expanded hole in 15 mm thick specimen

expanded holes. There are no significant differences in the average lives of the non-cold-expanded hole specimens in thicknesses of 15, 23 and 30 mm; nor are the differences in average lives significant for specimens of tnese thicknesses with cold-expanded holes. However, it should be noted that the average life of the 8 mm thick non-cold-expanded hole specimens is significantly greater (at a 5% level of significance) than those of the corresponding specimens in the 15 and 23 mm thickness (but not the 30 mm thickness); while that of the 8 mm thick cold-expanded hole specimens is significantly less than those of the other three thicknesses. This behaviour for non-cold-expanded hole specimens agrees with other work[18] on thickness effects in fatigue which attribute the differences to a transition from plane stress to plane strain conditions. However, it is not clear why the reverse appears with the cold-expanded hole specimens.

The multiple nature of fatigue crack initiation through the thickness (which has also been reported by Sanford et al[11]) was clearly shown in the residual strength specimens. Furthermore, in the current tests, the cracks at the mandrel entry face did not initiate at the corner of the hole but at a small distance down the bore (Figure 8(a)), whereas at the mandrel exit face they initiated at the corner of the hole (Figure 8(b)). However

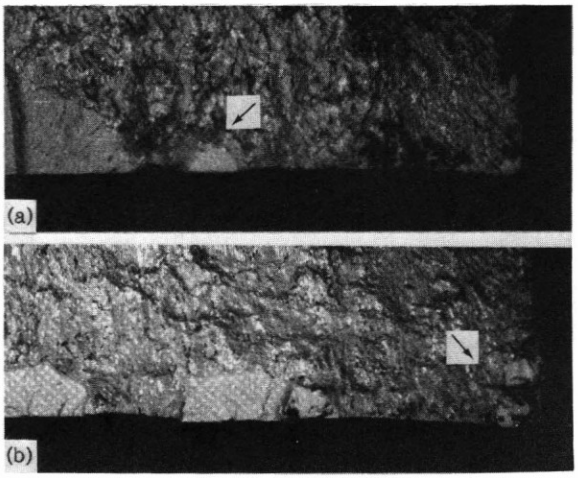

FIGURE 8. Fatigue crack initiation at (a) near inlet end of hole and (b) outlet end of hole in 15 mm thick specimen. Magnification x45

by about 40% to 50% of the life to failure, the crack development was relatively uniform in depth in the through-thickness direction. This general behaviour is reflected in the crack propagation curves shown in Figure 7. It appears that the development of the bulbous nose adjacent to the mandrel entry face occurs by accelerated crack growth during about the last one-third of the life. However, it is of interest to note from Table 4 that the maximum depth of the bulbous nose occurs some distance from the entry face, the actual distance apparently being thickness dependent. This is likely to be a reflection of the observation that, at the mandrel entry end of the hole, crack initiation did not occur at the corner of the hole.

It is suggested that the accelerated crack growth occurs when the crack front starts to progress through a decreasing hoop stress field. As the numerical values of the compressive hoop stress have been shown to be greater at the exit than the entry face[19], it is expected that the crack acceleration will first be manifested near the entry face. The reason for the maximum crack depth being between about 4 and 5 mm from the entry face is believed to be associated with the non-uniform stress field in the thickness direction.

The lack of agreement between the microhardness measurements and microstructural studies in this investigation and those reported in Reference 15 are likely to be associated firstly, with the combination of hole diameter (6 mm) and sheet thickness (3 mm) used in the latter, compared with a hole diameter of about 8.5 mm and specimen thickness of 15 mm in the present case. It is believed that the 3 mm thick sheet would provide less resistance to plastic deformation in the through-thickness direction because of the lack of plastic constraint. Secondly, the tests covered by Reference 15 involved much higher degrees of expansion (i.e. about 6% to 8% compared with about 4%). It has been shown by Gibson et al[20] (for about 6 mm diameter cold-expanded holes in 6.4 mm thick 7175 aluminium alloy) that it was only at cold expansions of about 5% and greater that microstructural changes adjacent to the surface of the hole became apparent.

A comparison of Figures 3 and 4 suggests that, at failure, the areas of fatigue cracking are greater for cold-expanded hole specimens than for non-cold-expanded hole specimens. Figure 9 shows the relationship between

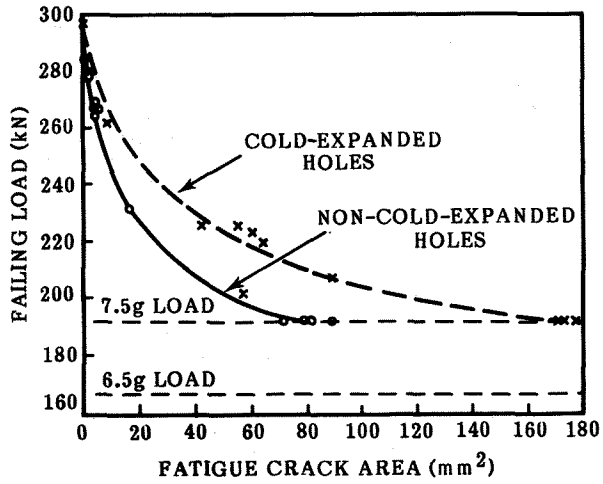

FIGURE 9. Residual strengths of 15 mm thick fatigue-cracked specimens

the failing loads and fatigue-cracked areas derived mainly from the residual strength tests. Although it was not possible to accurately measure the actual failing loads of specimens broken under fatigue loading, all of the cold-expanded hole specimens and half of the non-cold-expanded hole specimens failed during flight 42 of the 100-flight sequence. The continuous recording of the fatigue sequence indicated that, in such cases, the failing load was usually between 6.5 and 7.5g. However, relevant evidence is provided by the sizes of the cracks corresponding to the penultimate application of the +7.5g load to the various specimens, i.e. the crack sizes which can just be tolerated under this load magnitude. For the 15 mm thick non-cold-expanded hole specimens the fatigued areas ranged from 71 mm^2 to 88 mm^2, and for the cold-expanded hole specimens from 171 mm^2 to 176 mm^2. From Figure 9 it can be seen that the ratio of fatigue-cracked areas between cracked cold-expanded and cracked non-cold-expanded hole specimens is approximately two. These findings are of importance in damage and durability analyses. It is suggested that the compressive residual stresses induced by cold expansion, result in crack closure which reduces the effective stress intensity at the crack tip.

For 15, 23 and 30 mm thicknesses, the z-direction displacements at both the mandrel entry and exit faces are identical at distances exceeding about 3.5 mm from the edge of the hole. However, closer to the hole the z-direction displacements are, for all four thicknesses of material, smaller at the entry face than at the exit face - in both cases they are virtually the same for the 15, 23 and 30 mm thicknesses. These findings are generally consistent with those of Phillips[1] and Poolsuk and Sharpe[21], and again emphasise the fact that the expansion of the hole does not occur uniformly through the thickness. For example, in a 30 mm thick specimen, the actual changes in hole diameter at the mandrel entry face, half way through the hole and at the exit face were 2.6%, 2.2% and 2.8%. Additional evidence is provided by the change in width (along the length of the hole) of the ridge formed because of the split in the sleeve (see Table 7). Clearly, bell-mouthing of the hole occurs as reported by Schijve and Jacobs[22].

Thickness (mm)	Entry face average	Entry face s.d.	Mid-section average	Mid-section s.d.	Exit face average	Exit face s.d.
8	1.00	0.06	0.78	0.06	0.98	0.06
15	1.05	0.08	0.78	0.05	1.12	0.07
23	1.04	0.08	0.75	0.09	1.14	0.06
30	1.06	0.03	0.77	0.03	1.25	0.01

TABLE 7. Width (in mm) of ridge (at top) formed by the split in the sleeve. Results are from four of each thickness

Furthermore, the z-direction displacements in the 8 mm thick specimens are significantly less than for those of 15, 23 and 30 mm thickness at both the entry and exit faces. When considering the passage of the mandrel through the hole (particularly in a thick section) it could be postulated that the z-direction displacement at the entry face is the result of back-extrusion, while that at the exit face is caused by forward-extrusion.

For specimens of each of the four thicknesses, plots similar to those shown in Figures 6(a) and (b) were generated. It is apparent from these plots that the peak values of strain (particularly for the innermost gauges) do not occur at the same mandrel insertion distance for all hoop and radial gauges. Furthermore, peak values for corresponding hoop and radial gauges (i.e. those at equal distances from the hole edge) occur at mandrel insertion

distances separated by up to 2.5 mm. Such a result would not be expected in the case of pure radial hole expansion which is the situation usually modelled theoretically[23]. On the other hand, the standard FTI mandrel used in the present study had a maximum diameter parallel length of about 2.2 mm, considerably less that even the smallest specimen thickness of 8 mm. It would therefore not generate pure radial expansion simultaneously through the thickness, and it might be expected that any consequences of this would be thickness-dependent up to some limit defined by the geometry of the mandrel and the aspect ratio of the hole.

Lowak[24] has carried out fatigue tests on geometrically similar specimens of aluminium alloy AlCuMg2 having cold-expanded holes of 2, 4, 8 and 16 mm diameter, with corresponding thicknesses of 1.25, 2.5, 5 and 10 mm, i.e. an aspect ratio of 0.625. In every case the mandrel maximum diameter parallel section was twice the specimen thickness. He also gave the results of a strain analysis on a specimen with a 16 mm diameter hole, using linear gauge arrays similar to those in the present study. Use of a mandrel parallel section greater than the specimen thickness gives a closer approximation of pure radial expansion than was achieved in the current work. Lowak reported no lack of coincidence of gauge maximum readings and presents a simple formulation to calculate the residual stress field based on maximum and residual strain readings, i.e. mandrel fully inserted and completely withdrawn. Applying the Lowak formulation to the current strain readings results in a derived residual stress field which, although in substantial agreement with measured and theoretical values remote from the hole edge[2], are unrealistic within 1 to 2 mm of the hole where positive radial stresses are calculated. It is suggested that this problem may be a manifestation of the large z-direction displacements measured in this region (see Figure 5) or a consequence of a Bauschinger effect as suggested in Reference 25.

In the present study all cold-worked holes were expanded to between 4.0% and 4.2%. For each of the four thicknesses, the values of the hoop strain maxima are within a range of 20% with a tendency for the largest strains to occur in the 23 mm thick specimens. The range of residual strain values is greater (up to 80% difference between the 8 mm and 23 mm thick specimens being recorded) again with the greatest values occuring in the 23 mm thick specimens. For the four thicknesses, the range of both the maximum and residual radial strain values for the five gauges closest to the hole was usually less than 20%, with peak values occurring for either the 23 or 30 mm thickness. Similarly, radial strain readings for the outermost five gauges showed little variation of maximum readings; however there are considerable differences in the residual strains between the 8 mm and 23 mm thick specimens, increasing to a factor of 2 for the gauge furthest from the hole, the 23 mm thick specimen strain being highest.

The maximum and residual strain values have been plotted as a function of radial distance from the hole in Figure 10 for comparison with numerically derived values[26]. These strains were calculated for a hole aspect ratio of one; the measured strains correspond to an 8.4 mm hole in an 8 mm thick specimen. Although the calculated 'hole loaded' and 'hole unloaded' strains are about 30% to 40% higher than the measured values, the variations with radial distance from the hole show good agreement. The absolute differences may result from the assumed pure radial expansion implicit in the theoretical analysis compared to the effectively incremental expansion along the hole associated with the mechanic mandrel having a small length of maximum diameter.

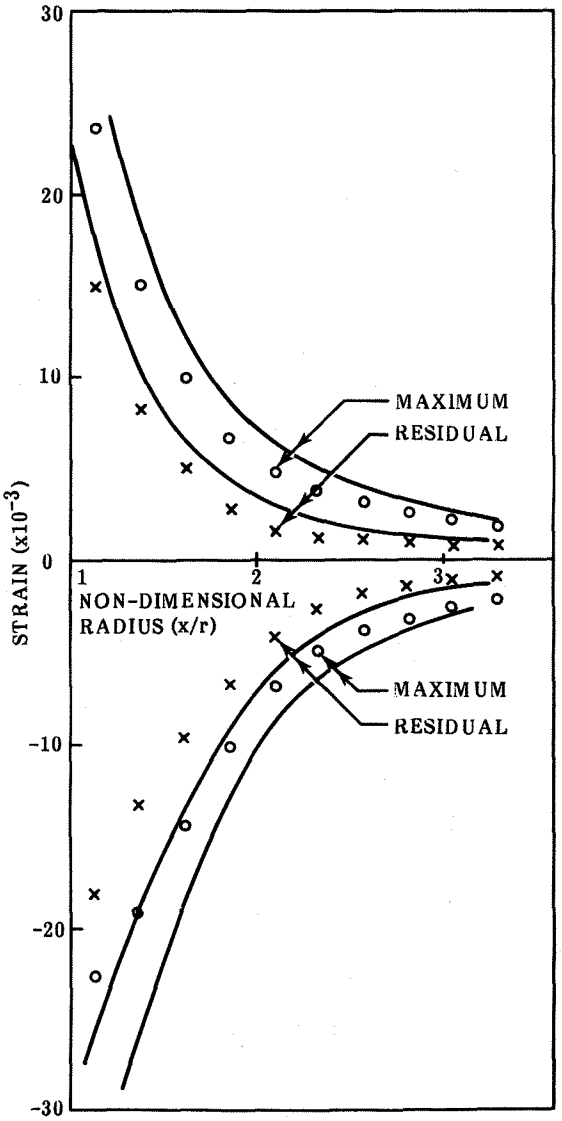

FIGURE 10. Predicted and measured values of maximum and residual strains (x = distance from hole, r = hole radius)

Three-dimensional theoretical derivation leads to identical z-direction displacements on the faces at both ends of the hole. As seen in Figure 11 the predicted value at the hole edge compared well with the average of the two measured values for the 8 mm thick specimens, although the calculated displacement extends further from the hole than was measured. Measurement of the radial distance corresponding to the onset of z-direction displacement has been used to identify the elastic-plastic boundary, at which point two-dimensional theory would predict that the hoop and radial strains should be of equal magnitude but of opposite sign[21]. In the present case, the measured onset of z-direction displacements occurs at approximately 5 mm from the edge of the hole for the 8 mm thick specimen and at about 8 mm from the edge for the other three thicknesses. This is in general accord with the findings of Carey [23,26] who calculated a smaller elastic-plastic radius for plane stress compared with plane strain conditions. The three-dimensional calculations, which are currently available only for a hole aspect ratio of one, are consistent in that both indicators relate to a boundary of x/r = 2 (4.3 mm from the hole edge in a 8 mm thick specimen).

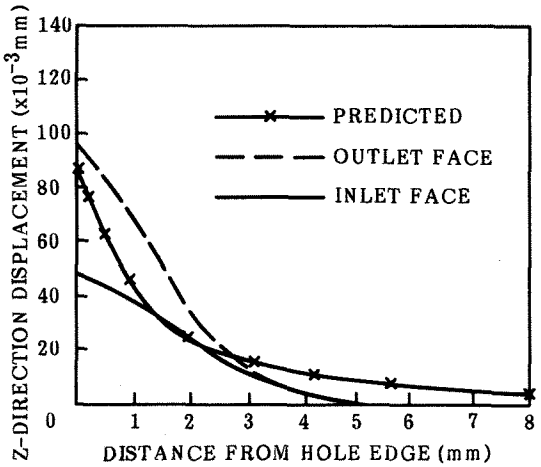

FIGURE 11. Comparison of predicted and measured out-of-plane displacements

Figures 6(a) and (c) indicate that the peak hoop strains at the innermost gauge occur when the maximum diameter parallel section of the madrel has fully entered the hole (indicated by arrow B). Most noticeable for the 8 mm thick specimen and effectively absent from the 30 mm thick specimen is the hoop strain minimum which occurs when the mandrel maximum diameter first begins to exit the hole (arrow C). When the maximum diameter parallel section has completely passed through the hole (arrow D) the hoop strains increase to their residual values. There is no equivalent minimum in the radial strain readings. The decrease in hoop strain at the entry face results from the elastic recovery of the material on which is superposed a compressive strain resulting from the moment generated by the offset loading applied by the mandrel parallel section as it traverses through the hole. When the mandrel maximum diameter fully exits the hole the removal of the moment gives rise to the observed increase in hoop strain.

V. CONCLUSIONS

This investigation has confirmed that significant improvements in fatigue life (by factors of four to six) can be achieved in an aircraft structural aluminium alloy by cold expansion. It was shown here that the life improvement is greater in thick than in thin sections.

Strain and displacement measurements associated with cold expansion have indicated large differences in the deformation characteristics and fatigue crack development at the mandrel entry and exit faces of the material, and that such differences are thickness dependent. One of the characteristics of fatigue crack development in thick sections containing holes with aspect ratios (length/diameter) exceeding about two is rapid fatigue crack growth near the mandrel entry face in the last 30% of the life, which leads to the formation of a bulbous crack front.

It has been shown that for a particular applied load a fatigue-cracked cold-expanded-hole specimen can tolerate a larger cracked area than a cracked non-cold-expanded hole specimen. In this investigation the ratio of cracked areas was approximately two.

These findings relating to fatigue life improvement, crack propagation characteristics and residual strength of fatigue-cracked specimens have some important implications in the implementation of damage-tolerance philosophies to aircraft structures incorporating cold-expanded holes.

REFERENCES

1. Phillips, J.L. Fatigue improvement by sleeve cold working. SAE. Pap. no. 730905, 1973.

2. Mann, J.Y. and Jost, G.S. Stress fields associated with interference-fitted and cold-expanded holes: with particular reference to the fatigue life enhancement of aircraft structural joints. Metals Forum, vol. 6, no. 1, 1983, pp. 43-53.

3. Mann, J.Y.; Machin, A.S. and Lupson, W.F. Improving the life of the Mirage IIIO wing main spar. Aust. Aeronaut. Res. Labs Struct. Rep. no. 398, Jan. 1984.

4. Mann, J.Y.; Machin, A.S.; Lupson, W.F. and Pell, R.A. Techniques for increasing the fatigue life of thick-section aluminium-alloy bolted joints. Aluminium, vol. 60, no. 7, July 1984, pp. 515-520.

5. Mann, J.Y.; Machin, A.S. and Lupson, W.F. Further investigations to improve the fatigue life of the Mirage IIIO wing main spar. Aust. Aeronaut. Res. Labs Struct. Tech. Memo. no. 397, Jan. 1985.

6. Mann, J.Y. and Kennedy, K.J. A case study in fatigue life extension - the main spar of RAAF Mirage IIIO wings. Mech. Engng Trans. I.E. Aust., vol. ME10, no. 2, July 1985, pp. 90-97.

7. Brot, A. Fatigue life evaluation program for the Kfir aircraft. Proc. 26th Israel annual conference on aviation and astronautics. 1984, pp. 36-42.

8. Beaver, P.W.; Mann, J.Y. and Sparrow, J.G. Fatigue life enhancement by the cold-expansion of holes - research and case study. Fatigue prevention and design. [Editor: J.T. Barnby]. Engineering Materials Advisory Services Ltd, 1986, pp. 123-136.

9. Mann, J.Y.; Sparrow, J.G. and Beaver, P.W. Fatigue characteristics of joints with holes cold-expanded in a multi-layer stack. [Submitted to International Journal of Fatigue, 1988.]

10. Hocker, R.G. Split-sleeve, cold worked holes in 7075-T73651 aluminium plate for improved life. Northrop Corp. Aircraft Div. Rep. no. NOR-82-80, Aug. 1982.

11. Sanford, R.J.; Graham, S.M. and Link, R.E. The mechanics of cold expanded fastener holes in 7075-T651 aluminium. Uni. Maryland Dept. Mechanical Engng Rep., Oct. 1986.

12. Mann, J.Y. and Revill, G.W. A comparison of fatigue lives under a complex and a much simplified flight-by-flight testing sequence. Aust. Aeronaut. Res. Labs Struct. Tech. Memo. no. 388, Aug. 1984.

13. Forsyth, P.J.E. Microstructural changes that drilling and reaming can cause in the bore holes in DTD 5014 (RR58) extrusions. Aircr. Engng, vol. 44, no. 11, Nov. 1972, pp. 20-23.

14. Leadbeater, G.; Noble B. and Waterhouse, R.B. The fatigue of an aluminium alloy produced by fretting on a shot peened surface. Fracture 84. 1986, pp. 2125-2132.

15. She Gong-Fan; Chen Yong and Chen Yan. Cold expanding of holes improves fatigue-life of aluminium alloy components. Fatigue prevention &

design. (Editor: J.T. Barnby]. Engineering Materials Advisory Services Ltd, 1986, pp. 99-106.

16. Morris, L.R.; Kenny, L.D. and Ryvola, M.A. Metallographic examination of the failure of thin sheet during bending. Microstructural science. [Editors: I. Le May and others]. Elsevier North Holland, 1979, vol. 7, pp. 59-67.

17. Pell, R.A.; Beaver, P.W.; Mann, J.Y. and Sparrow, J.G. Fatigue crack propagation from cold-expanded holes. [To be published]

18. Nathan, A.; Benoualid, D. and Brot, A. The effect of thickness on crack growth rate. New materials and fatigue resistant aircraft design. [Editor: D.L. Simpson]. Warley: Engineering Materials Advisory Services Ltd, 1987, pp. 283-296.

19. Noronha, P.J.; Henslee, S.P.; Gordon, D.E.; Wolanski, Z.R. and Yee, B.G.W. Fastener hole quality. U.S. Air Force Syst. Comm. Air Force Flight Dyn. Lab. Tech. Rep. no. AFFDL-TR-78-206, vol. 1., Dec. 1978.

20. Gibson, H.S.; Trevillion, C.G. and Faulkner, L. Thick section aluminium hole cold working. U.S. Air Force Materials Lab. Tech. Rep. no. AFML-TR-78-74, May 1978.

21. Poolsuk, S. and Sharpe, W.N. Measurement of the elastic-plastic boundary around coldworked fastener holes. J. Appl. Mech., vol. 45, Sept. 1978, pp. 515-520.

22. Schijve, J and Jacobs, F.A. Programme-fatigue test on aluminium alloy lug specimens with slotted holes and expanded holes. Netherlands Natl Lucht-Ruimtevaart Lab. Rep. no. TN M. 2139, Nov. 1964.

23. Carey, R.P. Computed stress and strain distributions under interference fit and after coldworking. Aust. Aeronaut. Res. Labs Struct. Tech. Memo. no. 466, Aug. 1987.

24. Lowak, H. Zum Einfluss von Bauteilgroesse, Lastfolge und Lasthorizont auf die Schwingfestigkeitssteigerung durch mechanisch erzeugte Druckeigenspannungen. Fraunhofer-Inst. Betriebsfestigkeit Ber. no. FB-157, 1981.

25. Amalbert, C.; Cornuault, C. and Thibaud, T. Modelling and analysis of the effect of "coldworking" on fatigue life. New materials and fatigue resistant aircraft design. [Editor: D.L. Simpson]. Warley: Engineering Materials Advisory Services Ltd, 1987, pp. 445-463.

26. Carey, R.P. Three-dimensional computation of stress, strain and strain energy density under interference-fit and after cold-working of holes. Aust. Aeronaut. Res. Labs Struct. Tech. Memo. no. 478, Jan. 1988.

ACKNOWLEDGEMENTS

The authors wish to acknowledge the assistance provided by Messrs L. Gratzer, L.I.M. Mirabella, M. Papaspiros and R.A. Pell during the course of this investigation.